Sound from rotors near a trailing edge

Michael Carley
Department of Mechanical Engineering
University of Bath
Bath BA2 7AY
United Kingdom
m.j.carley@bath.ac.uk

February 28, 2022

Abstract

A method of noise reduction proposed for the next generation of aircraft is to shield noise from the propulsion system, by positioning the noise source over a wing or another surface. In this paper, an approximate analysis is developed for the acoustic field far from a circular source placed near the edge of a semi-infinite plate, a model problem for shielding of noise by a wing and for scattering by a trailing edge. The approximation is developed for a source of small radius and is found to be accurate when compared to full numerical evaluation of the field.

1 Introduction

The effect of airframe configurations on the propagation of noise from propulsion systems is a question which has been studied over a number of years. In particular, studies have been conducted of the possibility of positioning propulsion systems in such a way that the airframe acts to "shield" the noise source and reduce noise levels reaching the ground. One example is the "Silent Aircraft" Initiative, in which a study was conducted of the scattering of noise from sources placed above the blended wing body configuration [1]. Another study [2] examined the effect of propeller positioning on an otherwise conventional airframe, making use of the tailplane for acoustic shielding. As electric propulsion improves, and novel configurations using airframe shielding for noise reduction become more feasible, there is a greater need for reliable methods which can be used in design and to provide insight into the propagation of sound around airframes.

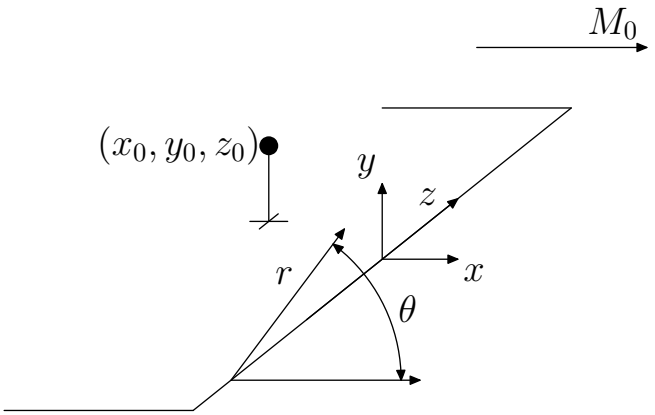

Figure 1: Notation for semi-infinite plate scattering

In this paper, we consider a rotating source located near the trailing edge of a semi-infinite plate in a uniform flow, a model problem for shielding of noise from over-wing rotors. In a study of shielding of noise from a counter-rotation open rotor [3], two theories for shielding attenuation were compared to experimental data, barrier theory and half-plane diffraction. It was found that neither gave accurate results, over-predicting the attenuation by $5\mathrm{dB}$ when a point source was used to approximate the rotor.

We present here an analysis of far-field noise from a rotating source which is comparable in its methods to established theory for noise from rotating sources, and which compares well to full numerical evaluation. It should be useful to designers and researchers as a starting point for parametric studies of rotor positioning in new configurations.

2 Analysis

The problem of scattering by a semi-infinite plane is an old one [4], which has been extended to include the effect of mean flow in the acoustic case [5]. We begin by presenting existing results for the problem in a form which can be incorporated into standard methods for the calculation of the acoustic far field of rotating sources.

2.1 Green's function

The coordinate system used to analyze the scattering of sound by a semi-infinite plate is shown in Figure 1. A uniform flow of Mach number M_0 is imposed normal to the trailing edge. A Cartesian coordinate system (x, y, z) is centred on the edge

of the plate, with x parallel to the flow, y normal to the plate and z aligned with the edge. A cylindrical coordinate system (r, θ, z) is defined, with $r = \sqrt{x^2 + y^2}$ and $\theta = \tan^{-1} y/x$. The Green's function for the field at a point (x, y, z) due to a source of time dependence $\exp[-\mathrm{i}\omega t]$ at (x_0, y_0, z_0) is given by [5]

$$G(\mathbf{x}, \mathbf{x}_0) = \frac{\mathrm{e}^{-\mathrm{i}KM_0(X-X_0)}}{\beta} \left[g_1(\mathbf{x}, \mathbf{x}_0) + g_2(\mathbf{x}, \mathbf{x}_0) \right], \tag{1}$$

$$g_i(\mathbf{x}, \mathbf{x}_0) = \frac{\mathrm{i}K}{8\pi} \int_{-\infty}^{S_i} \frac{H_1^{(1)}(K\overline{r}_i\sqrt{1+u^2})}{\sqrt{1+u^2}} \, \mathrm{d}u, \tag{2}$$

where $H_n^{(1)}(\,\cdot\,)$ is the Hankel function of the first kind, and

$$\begin{aligned}
\beta &= \sqrt{1 - M_0^2}, \quad X = \frac{x}{\beta}, \quad K = \frac{\omega}{c}\frac{1}{\beta}, \\
\overline{r}_{1,2} &= \left[(X - X_0)^2 + (y \mp y_0)^2 + (z - z_0)^2 \right]^{1/2}, \\
&= \left[\overline{r}^2 + \overline{r}_0^2 - 2\overline{r}\overline{r}_0 \cos\left(\overline{\theta} \mp \overline{\theta}_0\right) + (z - z_0)^2 \right]^{1/2}, \\
S_1 &= \frac{2\sqrt{\overline{r}\overline{r}_0}}{\overline{r}_1} \cos\frac{\overline{\theta} - \overline{\theta}_0}{2}, \quad S_2 = -\frac{2\sqrt{\overline{r}\overline{r}_0}}{\overline{r}_2} \cos\frac{\overline{\theta} + \overline{\theta}_0}{2}, \\
\overline{r} &= \sqrt{X^2 + y^2}, \quad \overline{\theta} = \tan^{-1}\frac{y}{X}.
\end{aligned}$$

For convenience, we note that the form of (1) is that of calculating the sound from a source and its image in the plane $y = 0$. If we take θ_1 as the coordinate of the source and define $\theta_2 = \theta_1 - 2\pi$ as the coordinate of the image, the acoustic field can be calculated as the sum of the fields g_i from the source and its image, using

$$\overline{r}_i = \left[\overline{r}^2 + \overline{r}_0^2 - 2\overline{r}\overline{r}_0 \cos\left(\overline{\theta} - \overline{\theta}_i\right) + (z - z_0)^2 \right]^{1/2}, \tag{3}$$

$$S_i = \frac{2\sqrt{\overline{r}\overline{r}_0}}{\overline{r}_i} \cos\frac{\overline{\theta} - \overline{\theta}_i}{2}. \tag{4}$$

We rewrite (2) in a form which facilitates physical interpretation when applied to the rotor noise problem, and can be used to efficiently approximate the field in different regions. Using the result

$$\int_0^\infty \frac{H_1^{(1)}(K\overline{r}_i\sqrt{1+u^2})}{\sqrt{1+u^2}} \, \mathrm{d}u = -\mathrm{i}\frac{\mathrm{e}^{\mathrm{i}K\overline{r}_i}}{K\overline{r}_i},$$

we can write g_i in a number of alternative forms,

$$g_i(\mathbf{x}, \mathbf{x}_0) = \frac{\mathrm{e}^{\mathrm{i}K\overline{r}_i}}{4\pi\overline{r}_i} - \frac{\mathrm{i}K}{8\pi}\mathcal{L}'(K\overline{r}_i, S_i), \tag{5}$$

$$= \frac{\mathrm{e}^{\mathrm{i}K\overline{r}_i}}{8\pi\overline{r}_i} + \frac{\mathrm{i}K}{8\pi}\mathcal{L}(K\overline{r}_i, S_i), \tag{6}$$

where for convenience, we define the functions

$$\mathcal{L}(\alpha, s) = \int_0^s \frac{H_1^{(1)}(\alpha\sqrt{1+u^2})}{\sqrt{1+u^2}}\,\mathrm{d}u, \tag{7}$$

$$\mathcal{L}'(\alpha, s) = \int_s^\infty \frac{H_1^{(1)}(\alpha\sqrt{1+u^2})}{\sqrt{1+u^2}}\,\mathrm{d}u. \tag{8}$$

The evaluation of the Green's function for scattering by the plate requires the evaluation of the integrals of (7) and (8). A solution for most of the far field will be found by approximating (8), while an exact expansion for (7) will be developed and used to find a solution for the remaining part of the field.

Integration by parts gives an asymptotic approximation for $\mathcal{L}'(\,\cdot\,)$,

$$\int_s^\infty \frac{H_1^{(1)}(\alpha\sqrt{1+u^2})}{\sqrt{1+u^2}}\,\mathrm{d}u \sim \frac{H_0^{(1)}(\alpha\sqrt{1+s^2})}{\alpha s}, \quad \alpha \to \infty, \tag{9}$$

so that for large $K\overline{r}_i$,

$$g_i(\mathbf{x}, \mathbf{x}_0) \approx -\mathrm{i}\frac{H_0^{(1)}(Kv)}{8\pi|\overline{r}_i S_i|} + \frac{\mathrm{e}^{\mathrm{i}K\overline{r}_i}}{4\pi\overline{r}_i} H(S_i), \tag{10}$$

$$v^2 = (\overline{r} + \overline{r}_0)^2 + (z - z_0)^2,$$

and $H(\,\cdot\,)$ is the Heaviside step function.

Integration by parts yields an approximation valid throughout the far field except as $|S_i| \to 0$ and allows us to interpret the Green's function in terms of the field generated by the source and by its image at $(x_0, -y_0, z_0)$. For all values of S_i, the first term in (10) contributes to the radiated field, corresponding to scattering from the edge. For points where $S_i > 0$, the free-field Green's function $\exp[\mathrm{i}K\overline{r}_i]/4\pi\overline{r}_i$ is "switched on" and contributes to the acoustic field. The acoustic domain can be decomposed into regions according to which terms of (10) contribute to the acoustic potential. Upon examination of the definition of S_i, it is clear that the boundaries of these regions are the lines through the trailing edge and the position of the source and of its image. Figure 2 shows these regions for a source placed above the plate, upstream of the trailing edge. Above the plate and for some distance behind it, both S_1 and S_2 are positive and the acoustic field can be viewed as that generated by the source and its image in the plate, with a correction term applied. Below the plate, where both S_1 and S_2 are negative, both free-field Green's functions are switched off and this region is a "shadow zone" where only the Hankel function of (10) contributes for each source. Finally, behind the trailing edge, in the wedge where $S_1 > 0$ and $S_2 < 0$, the main source contributes its free-field term, but the image source does not. A physical interpretation of the effect of

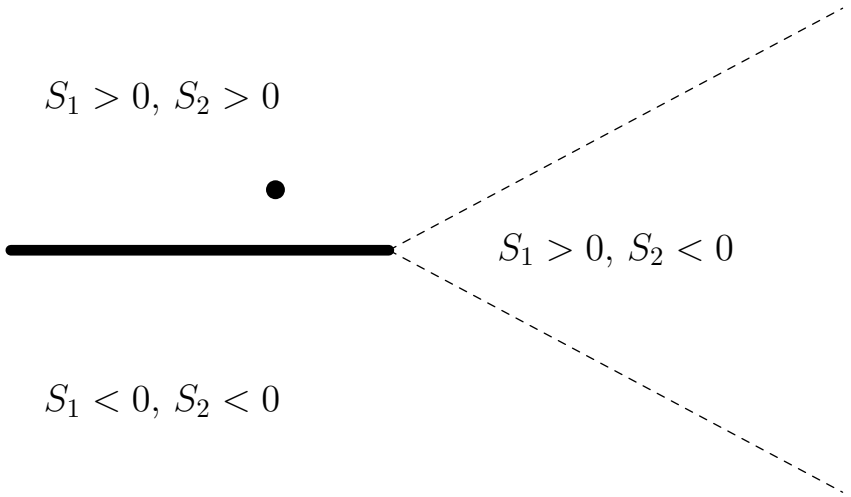

Figure 2: Contribution of acoustic source and image in different regions

$S_i \to 0$ is that the observer is approaching the line dividing the regions where a source does or does not contribute its free-field term, and g_i is better represented by (6).

In order to find an expansion which can be used for small S_i, we apply the product theorem for Bessel functions [6, 8.530.2] to (6),

$$\frac{H_1^{(1)}(\alpha\sqrt{1+u^2})}{\sqrt{1+u^2}} = 2\sum_{q=0}^{\infty}(-1)^q(2q+1)H_{2q+1}^{(1)}(\alpha)\frac{J_{2q+1}(\alpha u)}{\alpha u}. \tag{11}$$

Upon integration of the Bessel functions of the first kind,

$$\mathcal{L}(\alpha, s) = \frac{2}{\alpha}\sum_{q=0}^{\infty}(-1)^q H_{2q+1}^{(1)}(\alpha)\left[J_{2q+1}(\alpha s) + 2\sum_{k=1}^{\infty}J_{2q+2k+1}(\alpha s)\right], \tag{12}$$

which is exact for $|s| < 1$, though slow to converge as $|s| \to 1$. This result can be used to evaluate the acoustic field in the region $s \to 0$.

2.2 Acoustic field of a ring source near a trailing edge

We now apply the results of Section 2.1 to the estimation of the acoustic field of a rotating source impinging on the edge of a semi-infinite plate. The system is modelled as a ring source and its image in the plate, with the field of each calculated using the "partial" Green's function $G_{1,2}$ with

$$G_i(\mathbf{x}, \mathbf{x}_0) = \frac{\mathrm{e}^{-\mathrm{i}KM_0(X-X_0)}}{\beta} g_i(\mathbf{x}, \mathbf{x}_0) \tag{13}$$

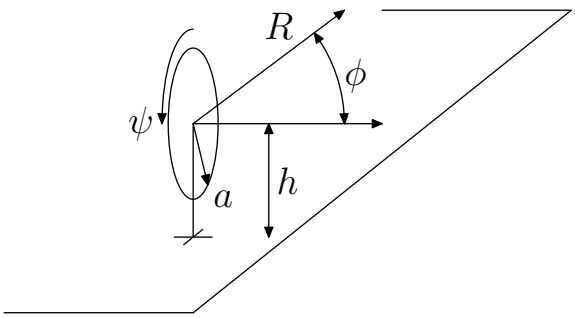

Figure 3: Coordinate system for evaluation of acoustic field of ring source

with the principal source denoted by subscript 1 and its image by subscript 2.

As is standard for rotor noise problems [7–11], the source is taken to vary as $\exp[\mathrm{i}n\psi_0]$ where ψ_0 is the angular variable on a circular source. To respect the image system, the image ring source has azimuthal variation $\exp[-\mathrm{i}n\psi_0]$ and its field can be calculated using the same analysis, changing n to $-n$.

The ring is centred at a point $(x_0, h, 0)$ with coordinates on the source given by

$$\mathbf{x}_0 = (x_0, h + a\cos\psi_0, a\sin\psi_0),$$

where a is the radius of the source. We introduce spherical coordinates centred on each ring source,

$$\begin{aligned} X - X_0 &= R_i\cos\phi_i, \\ y \pm h &= R_i\sin\phi_i\cos\psi_i, \\ z &= R_i\sin\phi_i\sin\psi_i. \end{aligned}$$

The acoustic field of each source is then given by

$$p_i(\mathbf{x}) = \frac{\mathrm{e}^{-\mathrm{i}KM_0(X-X_0)}}{\beta}\int_0^{2\pi}\mathrm{e}^{\mathrm{i}n\psi_0}g_i(\mathbf{x},\mathbf{x}_0)\,\mathrm{d}\psi_0. \tag{14}$$

We now develop an approximation for p_i valid in the far field. The first part of this calculation, for the effect of the free-field Green's function is well-known from previous work and is presented for completeness and to illustrate the approach taken.

We treat the field as made up of two contributions, corresponding to the "direct" field generated by the ring source, and that scattered by the trailing edge. The "ring" term is the familiar integral

$$\mathcal{R}_n(K, a, R_i, \phi_i, \psi_i) = \int_0^{2\pi}\frac{\mathrm{e}^{\mathrm{i}(K\overline{r}_i + n\psi_0)}}{4\pi\overline{r}_i}\,\mathrm{d}\psi_0, \tag{15}$$

for which a number of exact [11] and approximate [7, 9] expressions exist.

To evaluate the part of the field scattered by the trailing edge, we define the functions,

$$\mathcal{E}_n(K, a, \overline{r}_0, \overline{r}_i, S_i) = \frac{\mathrm{i}K}{8\pi} \int_0^{2\pi} \mathrm{e}^{\mathrm{i}n\psi_0} \mathcal{L}(K\overline{r}_i, S_i) \mathrm{d}\psi_0; \tag{16}$$

$$\mathcal{E}'_n(K, a, \overline{r}_0, \overline{r}_i, S_i) = \frac{\mathrm{i}K}{8\pi} \int_0^{2\pi} \mathrm{e}^{\mathrm{i}n\psi_0} \mathcal{L}'(K\overline{r}_i, S_i)\, \mathrm{d}\psi_0. \tag{17}$$

In the spherical coordinate system, $\overline{r}_i$ is given by

$$\begin{aligned} \overline{r}_i^2 &= R_i^2 + a^2 - 2a(y \mp h)\cos\psi_0 - 2az\sin\psi_0, \\ &= R_i^2 + a^2 - 2R_i a \sin\phi_i \cos(\psi_0 - \psi_i). \end{aligned}$$

Differentiating with respect to a and neglecting terms less than $O(1/R_i)$ yields a far-field approximation,

$$\begin{aligned} \overline{r}_i &\approx R_i - a\sin\phi_i\cos(\psi_0 - \psi_i), \\ \frac{1}{\overline{r}_i} &\approx \frac{1}{R_i}, \end{aligned}$$

which, upon insertion into (14) and use of tables [6, 8.411], yields the familiar result for the acoustic field of a ring source [7–9, among many others],

$$\mathcal{R}_n(K, a, R_i, \phi_i, \psi_i) \approx (-\mathrm{i})^n \mathrm{e}^{\mathrm{i}n\psi_i} \frac{\mathrm{e}^{\mathrm{i}KR_i}}{2R_i} J_n(Ka\sin\phi_i),$$

where $J_n(\,\cdot\,)$ is the Bessel function of the first kind. The free-field part of the ring-source field is then given by

$$p_i^{(f)}(\mathbf{x}) \approx \frac{\mathrm{e}^{-\mathrm{i}KM_0(X - X_0)}}{\beta} \mathcal{R}_n(K, a, R_i, \phi_i, \psi_i). \tag{18}$$

We can apply a similar approach to the approximation of the scattered field. Given

$$v^2 = \overline{r}_1^2(1 + S_1^2) = \overline{r}_2^2(1 + S_2^2) = (\overline{r} + \overline{r}_0)^2 + (z - z_0)^2,$$

to first order in a,

$$
\begin{aligned}
v &\approx v_0 + \frac{hSa}{v_0}\cos(\psi_0+\alpha),\\
v_0 &= \left[\left(\overline{r}+\sqrt{X_0^2+h^2}\right)^2 + z^2\right]^{1/2},\\
\alpha &= \tan^{-1}\frac{z/h}{1+\overline{r}/\sqrt{X_0^2+h^2}},\\
S^2 &= \left(\frac{\overline{r}}{\sqrt{X_0^2+h^2}}+1\right)^2 + \left(\frac{z}{h}\right)^2.
\end{aligned}
$$

Using Neumann's addition theorem [12, 10.23],

$$
\begin{aligned}
H_0^{(1)}(Kv) &\approx H_0^{(1)}\left(Kv_0 + \frac{KhSa}{v_0}\cos(\psi_0+\alpha)\right),\\
&= \sum_{q=-\infty}^{\infty} H_q^{(1)}(Kv_0)J_{-q}\left(K\frac{hSa}{v_0}\cos(\psi_0+\alpha)\right).
\end{aligned}
$$

With the use of tables [6, 6.681.8, 9], it is readily shown that for n and q both odd or both even, the integral

$$
\int_0^{2\pi} \mathrm{e}^{\mathrm{i}n\psi} J_q(\alpha\cos\psi)\,\mathrm{d}\psi = 2\pi J_{(q-n)/2}(\alpha/2)J_{(q+n)/2}(\alpha/2), \tag{19}
$$

and is identically zero otherwise. This yields

$$
\int_0^{2\pi} H_0^{(1)}(Kv)\mathrm{e}^{\mathrm{i}n\psi_0}\,\mathrm{d}\psi_0 \approx 2\pi\mathrm{e}^{-\mathrm{i}n\alpha}\sum_{q=-\infty}^{\infty} H_{2q+\delta}^{(1)}(Kv_0)J_{-(n'+q+\delta)}\left(K\frac{hSa}{2v_0}\right)J_{(n'-q)}\left(K\frac{hSa}{2v_0}\right),
$$

where $n = 2n' + \delta$, $\delta = 0, 1$.

The part of the ring-source field scattered by the trailing edge,

$$
\mathcal{E}_n'(K, a, \overline{r}_0, \overline{r}_i, S_i) = \frac{\mathrm{i}K}{8\pi}\int_0^{2\pi} \mathrm{e}^{\mathrm{i}n\psi_0}\mathcal{L}'(K\overline{r}_i, S_i)\,\mathrm{d}\psi_0,
$$

is then approximated by

$$
\mathcal{E}_n'(K, a, \overline{r}_0, \overline{r}_i, S_i) \approx -\frac{\mathrm{i}}{4}\frac{\mathrm{e}^{-\mathrm{i}n\alpha}}{\sqrt{v_0^2-R_i^2}}\sum_{q=-\infty}^{\infty} H_{2q+\delta}^{(1)}(Kv_0)J_{-(n'+q+\delta)}\left(K\frac{hSa}{2v_0}\right)J_{(n'-q)}\left(K\frac{hSa}{2v_0}\right). \tag{20}
$$

This approximation breaks down between the free-field being switched on or off where S_i is small ($v_0 \approx R_i$) and a different approximation is required in this region.

If the field point lies in a region which gives rise to small values of S_i in the integral of (14), the field must be evaluated using (12). Again, we proceed by approximating for the far field and using the properties of Bessel functions to find a form suitable for evaluation.

Returning to (12),

$$\mathcal{L}(\alpha, s) = \frac{2}{\alpha} \sum_{q=0}^{\infty} (-1)^q H_{2q+1}^{(1)}(\alpha) \left[J_{2q+1}(\alpha s) + 2 \sum_{k=1}^{\infty} J_{2q+2k+1}(\alpha s) \right],$$

and noting that $\alpha = K\overline{r}_i$, we seek an approximation which can be inserted into (14) and integrated. In the far field, $K\overline{r}_i \to \infty$, the difficulty lies in capturing the rapid variation in $K\overline{r}_i s_i$ as $s_i \to 0$. We proceed as follows to develop a tractable far-field approximation. The Hankel function is replaced by an approximation valid to first order in a, using the standard relations for derivatives,

$$H_m(K\overline{r}_i) \approx H_m(KR_i) + KaH_{m+1}(KR_i) \sin\phi_i \cos(\psi_0 - \psi_i) + O(1/(KR_i)^2).$$

The argument of the Bessel function of the first kind is approximated by

$$K\overline{r}_i s_i \approx 2K\sqrt{\overline{r}\overline{r}_0} \cos\frac{\overline{\theta} - \overline{\theta}_0}{2} + Ka\sqrt{\frac{\overline{r}}{\overline{r}_0}} \sin\frac{\overline{\theta} + \overline{\theta}_0}{2} \cos\psi_0,$$

and again using the product theorem [6, 8.530.2],

$$J_m(K\overline{r}_i s_i) \approx \sum_{k=-\infty}^{\infty} J_{m-k}\left(2K\sqrt{\overline{r}\overline{r}_0} \cos\frac{\overline{\theta} - \overline{\theta}_0}{2}\right) J_k\left(Ka\sqrt{\frac{\overline{r}}{\overline{r}_0}} \sin\frac{\overline{\theta} + \overline{\theta}_0}{2} \cos\psi_0\right),$$

yielding

$$\begin{aligned}\mathcal{L}(K\overline{r}_i, s_i) \approx \frac{2}{KR_i} \sum_{q=0}^{\infty} (-1)^q \left[H_{2q+1}^{(1)}(KR_i) + Ka \sin\phi_i H_{2q+2}^{(1)}(KR_i) \cos(\psi_0 - \psi_i) \right] \\ \times \left\{ \sum_{m=-\infty}^{\infty} J_m(\gamma_2 \cos\psi_0) \left[J_{2q+1-m}(\gamma_1) + 2 \sum_{k=1}^{\infty} J_{2q+2k+1-m}(\gamma_1) \right] \right\}, \end{aligned} \tag{21}$$

$$\gamma_1 = 2K\sqrt{\overline{r}\overline{r}_0} \cos\frac{\overline{\theta} - \overline{\theta}_0}{2}, \quad \gamma_2 = Ka\sqrt{\frac{\overline{r}}{\overline{r}_0}} \sin\frac{\overline{\theta} + \overline{\theta}_0}{2},$$

where all source coordinates such as $\overline{\theta}$ are evaluated at $a = 0$, the centre of the ring. Using (19), for $n = 2n'$,

$$\mathcal{E}_n(K, a, \overline{r}_0, \overline{r}_i, S_i) = \frac{\mathrm{i}K}{8\pi} \int_0^{2\pi} \mathcal{L}(K\overline{r}_i, s_i) \mathrm{e}^{\mathrm{i}n\psi_0} \, \mathrm{d}\psi_0 \approx$$

$$\frac{\mathrm{i}}{2R_i} \Bigg\{ \sum_{q=0}^{\infty} (-1)^q H^{(1)}_{2q+1}(KR_i) \sum_{m=-\infty}^{\infty} J_{m-n'}\left(\frac{\gamma_2}{2}\right) J_{m+n'}\left(\frac{\gamma_2}{2}\right) M_1(\gamma_1)$$

$$+\mathrm{e}^{-\mathrm{i}\psi_i} \frac{Ka\sin\phi_i}{2} \sum_{q=0}^{\infty} (-1)^q H^{(1)}_{2q+2}(KR_i) \sum_{m=-\infty}^{\infty} J_{m-n'}\left(\frac{\gamma_2}{2}\right) J_{m+n'+1}\left(\frac{\gamma_2}{2}\right) M_2(\gamma_1)$$

$$+\mathrm{e}^{\mathrm{i}\psi_i} \frac{Ka\sin\phi_i}{2} \sum_{q=0}^{\infty} (-1)^q H^{(1)}_{2q+2}(KR_i) \sum_{m=-\infty}^{\infty} J_{m-n'}\left(\frac{\gamma_2}{2}\right) J_{m+n'-1}\left(\frac{\gamma_2}{2}\right) M_3(\gamma_1) \Bigg\}, \tag{22}$$

where the auxiliary quantities are

$$M_1(\gamma_1) = J_{2(q-m)+1}(\gamma_1) + 2\sum_{k=1}^{\infty} J_{2(q+k-m)+1}(\gamma_1),$$

$$M_2(\gamma_1) = J_{2(q-m)}(\gamma_1) + 2\sum_{k=1}^{\infty} J_{2(q+k-m)}(\gamma_1),$$

$$M_3(\gamma_1) = J_{2(q-m+1)}(\gamma_1) + 2\sum_{k=1}^{\infty} J_{2(q+k-m+1)}(\gamma_1).$$

2.3 Summary

To summarize, the far-field sound from a rotor near the edge of a semi-infinite plane can be estimated by summing the contribution from the circular source of azimuthal order n and from its image in the plane, of order $-n$. For each source, the acoustic field is estimated by first determining the appropriate far-field approximation to apply. Figure 4 shows the region around a rotor divided according to the sign of S_i. In region I, $S_i > 0$ for all source positions on the rotor while in region II, $S_i < 0$. In region III, S_i changes sign for some value of ψ_0. The

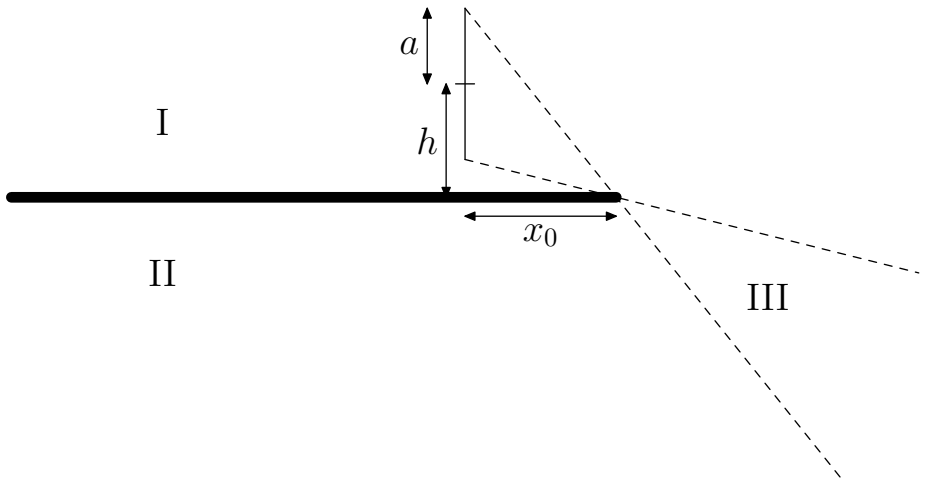

Figure 4: Regions around rotor labelled by far-field approximation

appropriate far-field approximation to use in each region is then:

$$p_n = \frac{\mathrm{e}^{-\mathrm{i}KM_0(X-X_0)}}{\beta}\left(\mathcal{R}_n - \mathcal{E}'_n\right), \qquad \text{(I)} \tag{23a}$$

$$= -\frac{\mathrm{e}^{-\mathrm{i}KM_0(X-X_0)}}{\beta}\mathcal{E}'_n, \qquad \text{(II)} \tag{23b}$$

$$= \frac{\mathrm{e}^{-\mathrm{i}KM_0(X-X_0)}}{\beta}\left(\frac{\mathcal{R}_n}{2} + \mathcal{E}_n\right), \quad \text{(III)}. \tag{23c}$$

In the far field, the functions $\mathcal{R}(\,\cdot\,)$, $\mathcal{E}(\,\cdot\,)$, and $\mathcal{E}'(\,\cdot\,)$ can be evaluated using the results given earlier. Finally, with regard to evaluation of the series defining these functions, we note that the Bessel function of the first kind $J_n(x)$ decays exponentially with increasing order for $n > x$, allowing the series to be truncated with negligible loss of accuracy.

3 Results

To illustrate the application of the method, we present sample results for an arbitrarily selected configuration, with rotor parameters $h = 0.9$, $a = 0.3$, $n = 6$. The rotor is positioned at $x_0 = -2a$, i.e. one rotor diameter upstream of the trailing edge. The rotor tip Mach number M_t is set to 0.6, so that the wavenumber $k = nM_t/a = 12$, and the flow Mach number $M_0 = 0.15$. The acoustic field is evaluated using the methods of this paper, and compared to full numerical evaluation, with results calculated above and below the plate to examine the shielding effect.

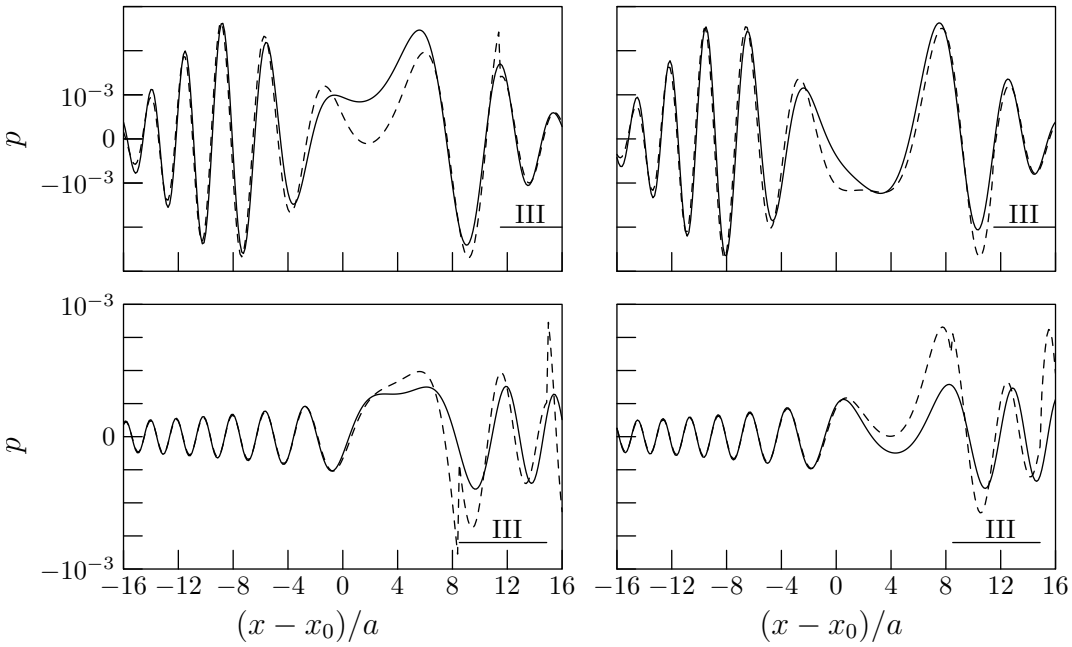

Figure 5: Acoustic potential above and below source; left-hand column: real part; right-hand column: imaginary part; solid line: numerical; dashed line: approximation.

Figure 5 shows the real and imaginary part of the potential at $-16a \leq x - x_0 \leq 16a$, $z = 0$, i.e. directly above and below the source centre. Results are calculated at a constant vertical displacement above and below the source, $y = h \pm 16a$. The region marked "III" on each plot shows where (23c) has been applied, in the transition region where the asymptotic approximation for the edge-scattered field breaks down. The beginning of this breakdown is apparent at the end of region III, in particular in the lower left-hand plot of the figure.

In applications, where the rotor may be placed above a wing in order to benefit from shielding effects, the region of interest is the "shadow zone" upstream of the trailing edge. The upper and lower fields are computed at constant distance from the source, so the different scales on the upper and lower plots make the shielding effect clear. In this case, the maximum amplitude upstream of the trailing edge is about ten times greater above the plate than below, and is well predicted by the far field approximation.

We note that while the results presented demonstrate good accuracy, the analysis is limited by the assumptions made in its development. In particular, the analysis does assume small source radius a and numerical experimentation has found that the accuracy of predictions degrades as a is increased. This may limit the applicability of the method, in particular as a becomes comparable to h, the

case of a rotor with a small tip clearance above the wing.

4 Conclusions

An approximate analysis has been developed for the radiation of sound from a rotating source near the edge of a semi-infinite plate in a uniform flow, a model problem for shielding and scattering of rotor noise by a wing. Sample calculations for small source radius show good agreement with full numerical evaluation, and capture the wing shielding effect reasonably accurately. Future work will focus on improving the accuracy and range of validity of the approximation, in particular in the case of small clearance between the rotor and wing. An open question is that of whether there is a useful exact expansion for the acoustic field, comparable to the series solutions which exist for isolated rotors.

References

[1] Anurag Agarwal and Ann P. Dowling. Low-frequency acoustic shielding by the Silent Aircraft airframe. *AIAA Journal*, 45(2):358–365, 2007.

[2] Petr Eret, John Kennedy, Francesco Amoroso, Paolo Castellini, and Gareth J. Bennett. Experimental observations of an installed-on-pylon contra-rotating open rotor with equal blade number in pusher and tractor configuration. *International Journal of Aeroacoustics*, 15(1–2):228–249, 2016.

[3] David B. Stephens and Edmane Envia. Acoustic shielding for a model scale counter-rotation open rotor. In *17th AIAA/CEAS Aeroacoustics Conference*, 2011.

[4] H. M. Macdonald. A class of diffraction problems. *Proceedings of the London Mathematical Society*, s2_14(1):410–427, 1915.

[5] Michel Roger, Stéphane Moreau, and Korcan Kucukcoskun. On sound scattering by rigid edges and wedges in a flow, with applications to high-lift device aeroacoustics. *Journal of Sound and Vibration*, 362:252–275, 2016.

[6] I. Gradshteyn and I. M. Ryzhik. *Table of integrals, series, and products*. Academic, London, 5th edition, 1980.

[7] L. Gutin. On the sound field of a rotating propeller. Technical Memorandum 1195, NACA, Langley Aeronautical Laboratory, Langley Field, Va. USA, 1948.

[8] I. E. Garrick and C. E. Watkins. A theoretical study of the effect of forward speed on the free-space sound-pressure field around propellers. Report 1198, NACA, 1953.

[9] S. E. Wright. Sound radiation from a lifting rotor generated by asymmetric disk loading. *Journal of Sound and Vibration*, 9(2):223–240, 1969.

[10] Michael Carley. Series expansion for the sound field of rotating sources. *Journal of the Acoustical Society of America*, 120(3):1252–1256, September 2006.

[11] Michael Carley. Series expansion for the sound field of a ring source. *Journal of the Acoustical Society of America*, 128(6):3375–3380, 2010.

[12] National Institute of Standards and Technology. Digital library of mathematical functions. `http://dlmf.nist.gov/`, 2010.